BIOCHEMISTRY
including biophysical chemistry & molecular biology

Current Topic

pubs.acs.org/biochemistry

Single-Molecule Dynamics and Mechanisms of Metalloregulators and Metallochaperones

Peng Chen,* Aaron M. Keller,† Chandra P. Joshi, Danya J. Martell, Nesha May Andoy,‡ Jaime J. Benítez,§ Tai-Yen Chen, Ace George Santiago, and Feng Yang

Department of Chemistry and Chemical Biology, Cornell University, Ithaca, New York 14853, United States

ABSTRACT: Understanding how cells regulate and transport metal ions is an important goal in the field of bioinorganic chemistry, a frontier research area that resides at the interface of chemistry and biology. This Current Topic reviews recent advances from the authors' group in using single-molecule fluorescence imaging techniques to identify the mechanisms of metal homeostatic proteins, including metalloregulators and metallochaperones. It emphasizes the novel mechanistic insights into how dynamic protein−DNA and protein−protein interactions offer efficient pathways via which MerR-family metalloregulators and copper chaperones can fulfill their functions. This work also summarizes other related single-molecule studies of bioinorganic systems and provides an outlook toward single-molecule imaging of metalloprotein functions in living cells.

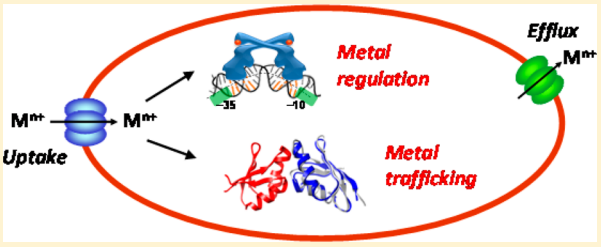

Transition metals, such as iron, copper, and zinc, play a variety of important roles in biological processes, including catalyzing reactions, providing structural supports, mediating charge transfer, and transducing signals.[1,2] Many transition metals are thus essential in organisms ranging from bacteria to mammals, yet some transition metals are highly toxic, such as mercury and lead, threatening organisms living in environments that contain high levels of such metals. Even essential metals can turn harmful if their concentrations and availabilities go awry inside cells. Therefore, it is crucial to understand how cells harness the power of essential metals for function, while preventing toxicity, and how they defend against toxic metals. This understanding is one of the major research goals in the field of bioinorganic chemistry (also known as inorganic biochemistry or metallobiochemistry), an active research field at the interface of chemistry and biology.

Most metal-related biological processes are conducted by proteins, i.e., metalloproteins. These proteins work either individually or with one another to conduct their biological functions. For the latter, the interactions among the proteins are often key determinants of their functionality. These interactions are often difficult to study in ensemble-averaged measurements because of their dynamic nature, which makes it necessary to synchronize molecular actions (as done in stopped-flow measurements) for probing interaction intermediates.

Single-molecule techniques have emerged over the past two decades as powerful methods for studying dynamic protein interactions (for example, see reviews 3−8). Their applications thrived in the field of biophysics: a quick look at the technical programs in the recent biophysics society national meetings can spot many lectures on single-molecule studies; examples include nucleic acid-processing enzymes, molecular motors, cytoskeleton structures, and protein synthesis and folding, to name a few. A search of the keywords "single molecule" and "biophysics" in PubMed generates >1500 publications. On the other hand, much less single-molecule studies have been reported on bioinorganic systems (see Related Single-Molecule Bioinorganic Work), even though bioinorganic chemistry is extensively intertwined with biology.[1,2] Yet many compelling problems in bioinorganic chemistry can be solved using the advances in single-molecule techniques, as shown by the examples in this work and others.

Approximately eight years ago, our group started an effort to develop and apply single-molecule fluorescence microscopy methods to bioinorganic problems, partly to target the shortage of this type of research as well as to push the frontiers of both bioinorganic chemistry and single-molecule research. We chose metal homeostasis as the topic of interest, which comprises many processes that involve dynamic protein−protein and protein−DNA interactions. Focusing on metalloregulators and metallochaperones, we have developed engineered DNA Holliday junctions as reporters in smFRET measurements of protein−DNA interactions, as well as adapted a lipid vesicle trapping approach to allow single-molecule studies of weak, dynamic protein interactions (see our previous review[9]). In this Current Topic, we highlight the mechanistic insights gained from our latest smFRET studies of metalloregulators and metallochaperones.

Received: May 13, 2013
Revised: July 23, 2013
Published: September 20, 2013

METALLOREGULATORS: NOVEL PATHWAYS FOR TRANSCRIPTION DEACTIVATION

Metalloregulators are metal-sensing transcription factors; they regulate the transcription of genes that protect the cell from metal excess or allow the cell to acquire essential metals (see recent reviews[10−26]). MerR-family metalloregulators make up a distinct family of these metalloregulators; they allow cells to sense and defend against many metal ions such as Hg^{2+}, Cu^{+}, and Zn^{2+}, with high selectivity and sensitivity. MerR, the archetype of the family, responds to Hg^{2+} and regulates the mercury resistance genes.[11,13,14,25,27−29]

How MerR-family metalloregulators activate transcription in response to metal ions has been well studied; they operate via a DNA distortion mechanism (Figure 1).[14,27,28,30,31] These

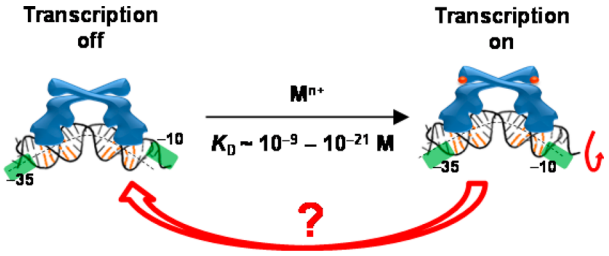

Figure 1. DNA distortion mechanism for transcription activation by MerR-family metalloregulators. The orange-colored base pairs denote the dyad symmetric sequence that the metalloregulator recognizes. The green shades denote the −10 and −35 elements of the promoter. The mechanism for transcription deactivation is unclear (red arrow).

homodimeric regulators recognize specific dyad symmetric DNA sequences within a promoter, and both their apo and holo forms bind DNA tightly. In the absence of metal, the metalloregulator bends the DNA; in this configuration, RNA polymerase (RNAp) cannot interact with both −10 and −35 sequences properly, and transcription is repressed. Upon binding metal, the metalloregulator changes its conformation and further unwinds the DNA slightly to allow proper RNAp interactions with the −10 and −35 sequences; transcription is then activated.

Until recently, little had been known about the mechanism by which MerR-family metalloregulators deactivate transcription (Figure 1). It is important, however, to deactivate transcription promptly, as it wastes energy for the cell to continue expressing metal resistance genes after metal stress is relieved. Dissociation of metal to convert a holo-metalloregulator to its apo form would be the simplest way to achieve deactivation but is unlikely, as the metal is bound tightly (often by cysteine ligands) and metal−cysteine bond dissociation is slow.[32] For example, CueR, the Cu^{+}-responsive MerR-family metalloregulator in *Escherichia coli*, has a Cu^{+} binding affinity of $\sim 10^{-21}$ M.[33] Although thiol ligand exchange can possibly facilitate the removal of Cu^{+} from the binding site as observed for copper chaperones,[34] no evidence exists that CueR can undergo similarly facile ligand exchange reactions. Then, to deactivate transcription, a holo-metalloregulator has to be either replaced somehow by its apoprotein or removed completely, which results in a vacant promoter that is also a weakly repressed state. Here, a simple scenario would be for the holoprotein to unbind from DNA, followed by the binding of an apoprotein, which will not only repress transcription but also prevent the rebinding of the holoprotein, but are there any alternative, and more efficient, pathways for deactivating transcription?

Using smFRET measurements, we have discovered novel pathways for transcription deactivation by MerR-family metalloregulators.[35] We focused on CueR, which regulates the transcriptions of CopA, a membrane transporter that pumps Cu^{+} out of the cytoplasm, and CueO, a periplasmic multicopper oxidase that is also involved in maintaining copper homeostasis.[36−39] In our experiment (Figure 2A), we immobilized on

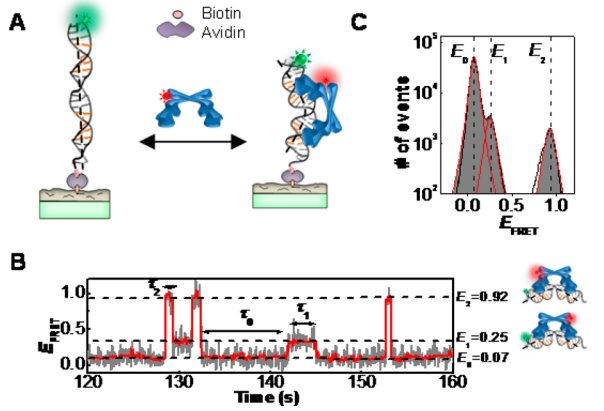

Figure 2. (A) Experimental scheme of surface immobilization of DNA. CueR is supplied in a continuously flowing solution. When CueR binds to DNA, FRET occurs from the donor Cy3 (green sphere) to the acceptor Cy5 (red sphere). (B) Single-molecule E_{FRET} trajectory of an immobilized Cy3-DNA interacting with holo-$CueR_{Cy5\text{-}C129}$ (2 nM), where Cy5-C129 designates the labeling position on one monomer. τ_0, τ_1, and τ_2 are the microscopic dwell times on the E_0, E_1, and E_2 states, respectively. The cartoons on the right show $CueR_{Cy5\text{-}C129}$ in two binding orientations. (C) Histogram of E_{FRET} trajectories as in panel B of holo-$CueR_{Cy5\text{-}C129}$−DNA interactions, showing the three E_{FRET} states.

a surface an oligomeric DNA (25 or 121 bp), which encoded the *copA* promoter sequence and was labeled at one end with a FRET donor Cy3 whose fluorescence was directly excited by a laser. We then allowed the protein molecule, which was labeled with a single FRET acceptor Cy5, to flow into the system. When protein binds to the DNA, FRET occurs from the donor to the acceptor, and the corresponding changes in the FRET efficiency [$E_{FRET} \approx I_A/(I_A + I_D)$, where I_D and I_A are the donor and acceptor fluorescence intensities, respectively] report the protein−DNA interactions. As CueR is a homodimer, labeling it with a single FRET acceptor breaks its symmetry. Consequently, its two orientations for binding onto DNA are differentiated. The E_{FRET} versus time trajectory from a single immobilized DNA interacting with proteins in solution shows transitions among three different E_{FRET} states: the E_0 state corresponds to the free DNA, and E_1 and E_2 correspond to the two different binding orientations of labeled CueR on DNA (Figure 2B,C).

Kinetic Mechanism of CueR−DNA Interactions and Its Functional Implications. Figure 3 gives the kinetic mechanism and the associated rate constants of apo- and holo-CueR interacting with a specific DNA that contains the dyad symmetric sequence recognized by CueR. The protein (P) binds to DNA (D) reversibly (k_1 and k_{-1} processes) to form a complex (I) in which CueR recognizes the specific sequence and distorts the DNA structure. The reversible binding processes are manifested experimentally by the

dx.doi.org/10.1021/bi400597v | *Biochemistry* 2013, 52, 7170−7183

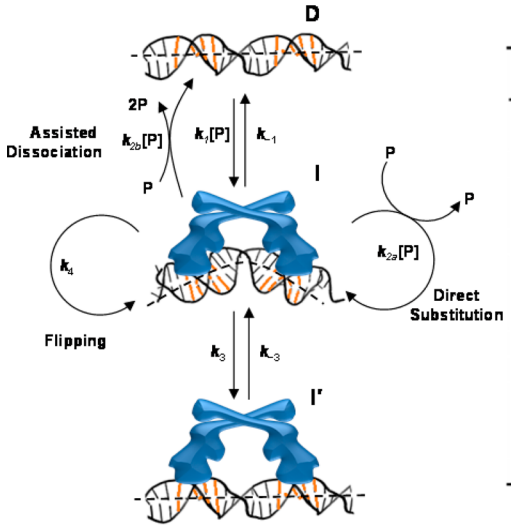

Processes	Kinetic parameters	Holo	Apo
Binding	k_1 (×10^6 M^{-1}s^{-1})	9 ± 4	6 ± 1
Unbinding	k_{-1} (s^{-1})	1.1 ± 0.3	0.4 ± 0.1
Dissociation constant	K_D (= k_{-1}/k_1) (nM)	122 ± 63	67 ± 20
Inter-conversion	k_3 (s^{-1})	2.0 ± 0.2	0.4 ± 0.1
	k_{-3} (s^{-1})	1.4 ± 0.1	0.54 ± 0.07
	K_{3D} = k_3/k_{-3}	1.4 ± 0.2	0.74 ± 0.2
Substitution	k_{2a} (×10^6 M^{-1}s^{-1})	134 ± 20	-
Assisted dissociation	k_{2b} (×10^6 M^{-1}s^{-1})	-	54 ± 22
Flipping	k_4 (s^{-1})	0.13 ± 0.05	0.21 ± 0.03

Figure 3. Kinetic mechanism of interactions of CueR with a specific DNA, which includes the protein (P), DNA (D), two protein–DNA complexes that differ in protein binding modes (I and I′), and the rate constants for the kinetic processes. [P] denotes the protein concentration. Between k_{2a} and k_{2b}, direct substitution process k_{2a} is dominant for holo-CueR–DNA interactions, whereas assisted dissociation process k_{2b} is dominant for apo-CueR–DNA interactions. The kinetic parameters are listed in the table. The rate constants for CueR (holo) binding and unbinding with nonspecific DNA are as follows: k_1 = 0.016 ± 0.001 nM^{-1} s^{-1}, and k_{-1} = 5.9 ± 0.1 s^{-1}. Other kinetic processes do not occur to nonspecific DNA.[35]

reversible transitions between E_0 and E_1 states and those between E_0 and E_2 states in the E_{FRET} trajectories (Figure 2B). The structural distortion of DNA in the CueR–DNA complex was well-known from the structural studies of other MerR-family regulators in complex with DNA.[14,27,30,31]

Interestingly, we observed that both apo- and holo-CueR could spontaneously flip their binding orientations on DNA without completely detaching from DNA [k_4 (Figure 3)]. This spontaneous flip is experimentally manifested by the direct $E_1 \leftrightarrow E_2$ transitions that can be observed down to protein concentrations as low as 0.5 nM (e.g., at ∼130 s in Figure 2B). Furthermore, this flipping occurs only when CueR binds to the specific DNA sequence, where CueR distorts DNA structure (complex I in Figure 3), as it is not observed in interactions of CueR with a nonspecific DNA.[35] Similar flipping behaviors were also observed for HIV reverse transcriptase on DNA–RNA duplexes.[40] This spontaneous flipping indicates that CueR is highly dynamic when bound at its recognition site on DNA. Being dynamic, especially for holo-CueR, may facilitate transcription initiation, which involves large structural rearrangements of associated proteins and DNA.[28]

We further discovered that for both apo- and holo-CueR, within each protein-binding orientation on DNA, there was another binding mode besides the one at which CueR recognized the targeting sequence and distorted the DNA structure; i.e., CueR has two different binding modes on DNA (I and I′ in Figure 3). These two different binding modes are experimentally manifested in the distribution of τ_2 (and the equivalent τ_1), the microscopic dwell time on the protein-bound E_2 state (Figure 2B). The distribution of τ_2 follows a double-exponential decay (Figure 4A). Furthermore, the two different modes of binding of CueR on DNA are present only when CueR recognizes the specific DNA sequence, because, when CueR interacts with a nonspecific DNA, the distribution of the dwell time on the protein-bound state follows a single-exponential decay.[35] We attributed the second CueR binding mode to a CueR–DNA complex in which the CueR binds DNA in a way as if the DNA is nonspecific; this attribution is reasonable because CueR does bind nonspecific DNA and the

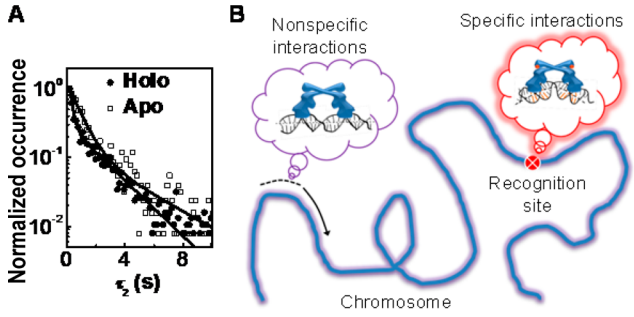

Figure 4. Two different modes of binding of CueR on specific DNA. (A) Double-exponential distributions of τ_2 for interactions of holo- and apo-CueR$_{Cy5\text{-}C129}$ with specific DNA, both at 2 nM protein. (B) Schematic of CueR sliding on a chromosome via nonspecific interactions to help search for the recognition site at which specific interactions apply.

binding mode here must be different from that of the specific DNA binding mode. No structural information is yet available about CueR, or any MerR-family regulators, in complex with a nonspecific DNA. For the purposes of illustration, we drew the cartoon of this complex having the DNA structure undistorted (I′ in Figure 3). The two different binding modes, in which CueR interacts with DNA specifically or nonspecifically, are beneficial for CueR in its searching for the recognition sequence in the large bacterial chromosome (∼4.6 million bp for *E. coli*[41]); being able to interact with DNA nonspecifically would help CueR slide along the chromosome, and upon locating the recognition sequence, the CueR–DNA complex can interconvert to the specific binding mode, thereby distorting the DNA structure to regulate transcription (Figure 4B). This sliding along DNA via nonspecific interactions has long been recognized as being advantageous for reducing the dimensionality of site search for DNA-binding proteins[42] and has been directly visualized via single-molecule tracking, for example, for an adenovirus proteinase.[43]

Most strikingly, we discovered that CueR could undergo two novel processes at the specific DNA site, both of which

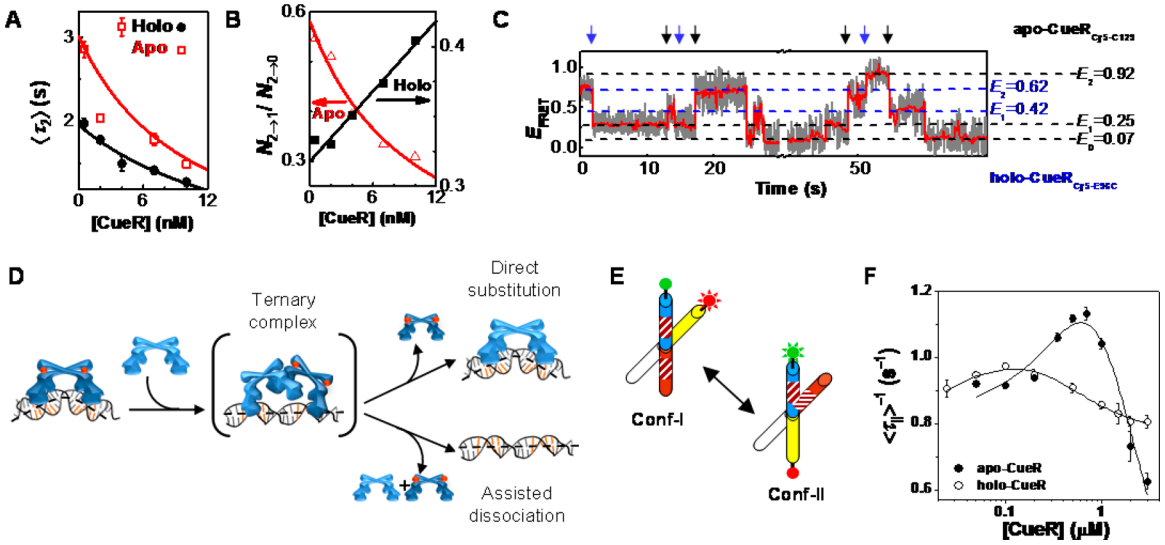

Figure 5. Direct substitution and assisted dissociation pathways of CueR–DNA interactions. (A) CueR concentration dependence of $\langle\tau_2\rangle$ for $CueR_{Cy5\text{-}C129}$–DNA interactions. (B) Dependence of $N_{2\to1}/N_{2\to0}$ on holo-$CueR_{Cy5\text{-}C129}$ and apo-$CueR_{Cy5\text{-}C129}$ concentrations. $N_{2\to1}/N_{2\to0}$ is the ratio of observed numbers of $E_2 \to E_1$ to $E_2 \to E_1$ transitions in E_{FRET} trajectories such as those in Figure 2B. (C) Single-molecule E_{FRET} trajectory of an immobilized Cy3-DNA interacting with a mixture of apo-$CueR_{Cy5\text{-}C129}$ and holo-$CueR_{Cy5\text{-}E96C}$ at 5 nM each. The blue arrows denote the transitions from the holoprotein-bound states to the apoprotein-bound states, and the black arrows denote the reverse transitions; these transitions report the direct substitution of a DNA-bound holoprotein by an apoprotein or the reverse. (D) Schematic of the proposed mechanism involving a ternary $CueR_2$–DNA complex as a common intermediate (or transition state) for the direct substitution and assisted dissociation to a CueR that is bound at the specific DNA site. Note here CueR is a homodimer. (E) Structural dynamics of an engineered Holliday junction (HJ) between its two conformers, conf-I and conf-II, with FRET donor (green) and acceptor (red) labels. The stripes on two arms indicate the encoded dyad symmetric sequence recognized by CueR. (F) CueR concentration dependences of $\langle\tau_{II}\rangle^{-1}$, where τ_{II} is the single-molecule dwell time on conf-II in E_{FRET} trajectories of HJ structural dynamics. Reprinted with permission from ref 45. Copyright 2009 Elsevier.

interrupt an existing CueR–DNA complex. In one, a direct substitution process, which is dominant for holo-CueR–DNA interactions, a protein coming from the surrounding solution directly replaces the incumbent protein on DNA [k_{2a} (Figure 3)]; in the other, an assisted dissociation process, which is dominant for apo-CueR–DNA interactions, a protein from solution helps carry away the incumbent one on DNA [k_{2b} (Figure 3)]. Both of these processes lead to a shortening of the average single-molecule dwell time (e.g., $\langle\tau_2\rangle$) of each protein-binding orientation when the holo- or apoprotein concentration increases (Figure 5A). (Note that overall, the protein still spends more time on DNA at higher protein concentrations because of the higher binding rates.)

However, clear differences between holo- and apo-CueR behaviors differentiate these two processes. For holo-CueR, at higher protein concentrations, more frequent transitions are observed between the two protein-binding orientations (Figure 5B), because direct substitution has a 50% probability that the replacing protein ends up in a binding orientation opposite from the incumbent one. In contrast, for apo-CueR, at higher protein concentrations, more frequent transitions are observed from a bound state to the free DNA state because of the assisted dissociation process (Figure 5B). Using two differently labeled CueR variants, each prepared in the apo or holo form, we further observed the direct substitution processes on a specific DNA between apo- and holo-CueR, reflected by the direct transitions from the bound states of one variant to those of the other (Figure 5C). Moreover, both k_{2a} and k_{2b}, the rate constants for direct substitution and assisted dissociation, respectively, are significantly larger than k_1, the protein binding rate constant; these larger rate constants indicate that the presence of a CueR on DNA facilitates the process of another CueR molecule finding the recognition sequence, leading to either direct protein substitution or assisted protein dissociation.

Similarly, Marko et al. have observed that some sequence-neutral DNA-binding proteins can readily exchange with themselves or with each other on DNA;[44] we hypothesize that the direct substitution or the assisted dissociation pathway could be the underlying mechanism for these facile protein exchanges on DNA. Besides being novel mechanistic pathways for protein–DNA interactions, these two pathways are also functionally significant for MerR-family metalloregulators, as will be discussed later.

Protein$_2$–DNA Ternary Complex as a Possible Intermediate (or transition state) for Direct Substitution and Assisted Dissociation Pathways. The direct substitution and assisted dissociation processes that occur to a CueR molecule bound at the specific DNA site pose an immediate question: how do they occur at the molecular level? Here we propose a mechanism that involves a protein$_2$–DNA ternary complex as a common intermediate (or transition state[a]) for both pathways [here each protein is a functional dimer of CueR (Figure 5D)]. Start with a CueR–DNA complex, in which each of the two DNA-binding domains of the homodimeric CueR attaches to one-half of the dyad symmetric sequence. Under thermal fluctuation, one of the DNA-binding domains could detach momentarily, allowing another CueR molecule to bind to one-half of the dyad with one of its DNA-binding domains and leading to a $CueR_2$–DNA ternary complex (note CueR is a homodimer dimer). Because of the low stability of the ternary complex, it could proceed in either of the two pathways. In one, the incumbent CueR falls off DNA, resulting in a direct substitution (the incoming one could fall off too, leading to no observable change). In the other, both proteins fall off, resulting in an assisted dissociation.

dx.doi.org/10.1021/bi400597v | *Biochemistry* 2013, 52, 7170–7183

A $CueR_2$–DNA ternary complex was indeed observed in our previous study,[45] where we used an engineered DNA Holliday junction (HJ) to probe CueR–DNA interactions. A DNA HJ is a four-way junction of DNA. In the presence of Na^+ and Mg^{2+}, it folds into two X-shaped stacked conformers [conf-I and conf-II (Figure 5E)], where each conformer could be viewed approximately as two B-form helices forming a cross structurally.[46,47] The two conformers interconvert dynamically at room temperature (Figure 5E), and the structural dynamics of a single HJ molecule can be followed in real time by smFRET measurement where two of the HJ's four arms are labeled with a FRET pair.[45,48−50] We engineered a HJ and encoded in its arms the dyad symmetric sequence recognized by CueR (Figure 5E). Because the part of HJ that contains the encoded sequence has distinct spatial orientations in the two conformers, CueR binds to the two conformers differentially and causes changes in the interconversion kinetics between the two conformers. These changes can be readily measured by smFRET and thus report the associated protein–DNA interactions.[45,49] We found that both apo- and holo-CueR interacted with conf-II in a two-step manner; they initially bind to conf-II to form a binary complex that can facilitate its structural transition to conf-I, and this binary complex can then bind a second protein molecule to form a ternary complex that stabilizes conf-II. The two-step interactions of CueR with conf-II are manifested by the biphasic protein concentration dependence of $\langle\tau_{II}\rangle^{-1}$, the time-averaged single-molecule rate of the conf-II → conf-I transition (Figure 5F); with an increasing CueR concentration, $\langle\tau_{II}\rangle^{-1}$ initially increases, reflecting the formation of the binary complex that aids in the structural transition to conf-I, and then it decays at higher protein concentrations after reaching a maximum, reflecting the subsequent formation of the ternary complex.

The observation of a ternary complex here likely results from that in the HJ conf-II; the spatial orientation of the two halves of the dyad symmetric sequence is significantly distorted from that in a double-stranded DNA helix (Figure 5E), allowing two CueR molecules to bind, each of which accesses one-half of the dyad sequence. In contrast, in a normal double-stranded DNA helix, its structural distortion upon CueR binding is small;[14,27,30,31] the small magnitude of this structural distortion likely renders the ternary complex unstable and merely a short-lived intermediate (or transition state), which nevertheless could provide a possible molecular mechanism for the direct substitution and assisted dissociation pathways observed experimentally.

Efficient Pathways for Transcription Deactivation and Their Broader Relevance. Besides being novel pathways in protein–DNA interactions, the direct substitution and assisted dissociation could both be functionally significant for deactivating transcription in CueR's regulatory function. For transcription deactivation, the holo-CueR-bound promoter needs to return to the apo-CueR-bound state or the free DNA form (Figure 1). The direct substitution of a holoprotein by an apoprotein can reach the apo-bound state in a single step: its kinetics depends on the intracellular concentration of CueR. Depending on growth conditions, an *E. coli* cell has approximately 60–400 copies of monomeric CueR,[51] corresponding to ≈30–220 nM P with a cell volume of ∼1.5 fL[33] (where P is the functional homodimer). Using rate constant k_{2a} (Figure 3), the direct substitution takes approximately 0.03–0.2 s to reach the apoprotein-bound, transcription-repressed state (Figure 6, step iii). On the other hand, the assisted dissociation

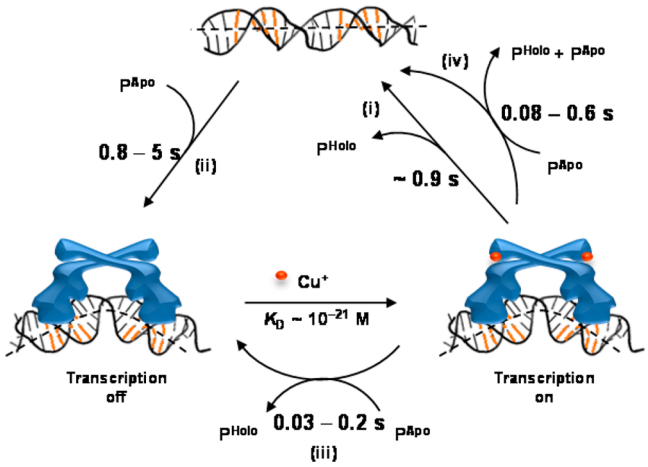

Figure 6. Pathways for transcription deactivation by CueR. The time scales are denoted for relevant kinetic steps, including (i) unbinding, (ii) binding, (iii) direct substitution, and (iv) assisted dissociation. P^{Apo} represents apo-CueR and P^{Holo} holo-CueR.

takes approximately 0.08–0.6 s to reach the free DNA form (Figure 6, step iv), using rate constant k_{2b}. Compared with the generic pathway of protein unbinding and binding (Figure 6, steps i and ii, total of approximately 1.7–5.9 s) or that of just unbinding (step i, ∼0.9 s), direct substitution and assisted dissociation are both tens of times faster. Therefore, both the direct substitution of holo-CueR by apo-CueR and the assisted dissociation of holo-CueR at the promoter site could be the more efficient pathways for transcription deactivation.

One expects that cellular conditions are possibly not the same as in our experiments, and kinetic constants may thus differ. The percentage of cellular CueR being holo or apo is not known under different copper exposures and growth conditions. The turnover rates of apo- and holo-CueR in cells could also provide another layer of control in affecting the kinetics of interaction of CueR with DNA. With these complications, the two novel pathways we discovered here do not prove that they must operate *in vivo*, but they can occur, making them possible mechanistic pathways for transcription deactivation.

Moreover, past studies have shown that for the archetype Hg^{2+}-responsive metalloregulator MerR, a protein called MerD might mediate the unbinding of holo-MerR from DNA for transcription deactivation,[25] a scenario analogous to assisted dissociation. No evidence has yet been found, however, for a MerD homologue of CueR or other MerR-family metalloregulators. As all known MerR-family metalloregulators share the DNA distortion mechanism for transcription activation,[14,27,30] it is thus reasonable to think that most of them share a common mechanism for transcription deactivation. Therefore, the direct substitution and assisted dissociation pathways, if operating, might be common mechanisms for MerR-family metalloregulators to deactivate transcription efficiently after transcription activation.

METALLOCHAPERONES: VERSATILE PATHWAYS FOR COPPER TRAFFICKING

Metallochaperones are transport proteins that deliver metal ions to their destinations or intermediate locations inside cells while protecting the metals from adventitious binding sites or harmful reactions.[52−56] In human cells, copper chaperone Hah1

(also named Atox1) delivers Cu^+, an essential but potentially harmful metal ion, to two homologous P_{IB}-type ATPases: the Wilson's disease protein (WDP) and Menkes disease protein (MNK), which use ATP hydrolysis to further drive translocation of Cu^+ through the membrane for either subsequent incorporation into copper enzymes or export.[52,57−59]

Both WDP and MNK have six N-terminal metal-binding domains (MBDs), connected by flexible peptides of various lengths (Figure 7). All these MBDs, as well as Hah1, are homologous, each with a $\beta\alpha\beta\beta\alpha\beta$ protein fold and a CXXC motif that binds Cu^+ with an affinity of $\sim 10^{18}$ M^{-1}.[60−65] Under a shallow thermodynamic gradient, Hah1 can transfer Cu^+ to each MBD,[61,66] and the transfer is mediated by weak and dynamic protein interactions and involves metal bridging of the CXXC motifs of the two proteins.[52,57,59,67−70]

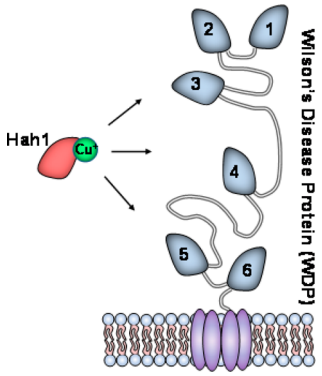

Figure 7. Schematic of trafficking of Cu^+ from Hah1 to the six MBDs of WDP (or MNK) anchored on a membrane.

Both intermolecular Hah1−MBD interactions and intramolecular MBD−MBD interactions are vital to the transport of copper from Hah1 to WDP/MNK. The multiplicity of the WDP/MNK MBDs also seems important because the number of MBDs, which varies between one and six in homologous proteins,[71,72] tends to be larger for higher organisms (for example, yeast homologue Ccc2 has merely two MBDs[73]). Characterizing and understanding these interactions are thus an important tasks but are challenging. Surface plasmon resonance has been used to study the kinetics of these interactions,[74,75] but the nonspecific protein−surface interactions therein may perturb the kinetics. Nuclear magnetic resonance (NMR),[66,76−83] X-ray crystallography,[67,84−86] protein docking,[68] and molecular dynamic simulations[70,87−89] have provided detailed structural information about the interaction interfaces, but they only provided estimates of the interaction thermodynamics and kinetics.

To complement these studies while overcoming some of their limitations, we have used smFRET in combination with lipid vesicle trapping[90−93] to quantify weak and dynamic interactions between Hah1 and WDP MBDs.[93−96] In this approach, we label the two interacting partners with a FRET donor−acceptor pair and cotrap them within a surface-immobilized ~100 nm diameter unilamellar lipid vesicle. The FRET pair allows us to detect protein interactions at the single-molecule level, similar to the studies of metalloregulator−DNA

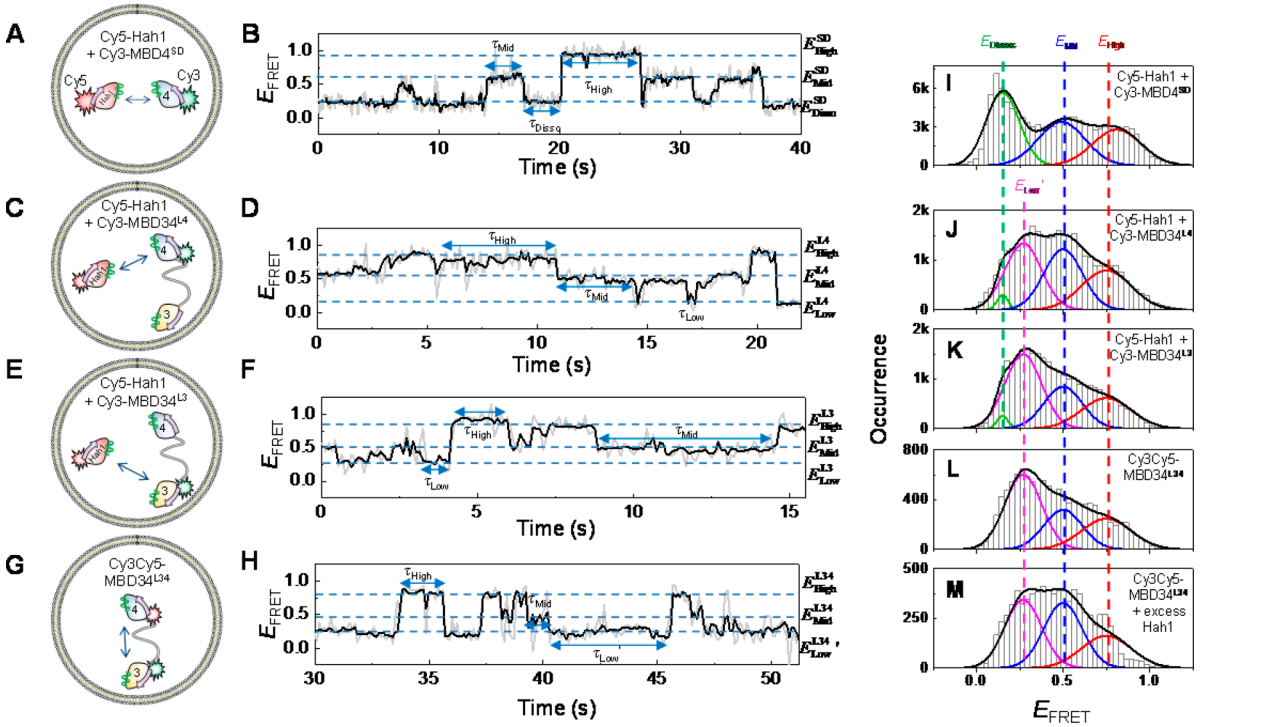

Figure 8. (A, C, E, and G) Protein labeling schemes for probing pairwise interactions. The lipid vesicles were immobilized on a surface for smFRET measurements. For the nomenclature, for example, in $MBD34^{L4}$, the L4 superscript denotes that the label is on MBD4 within MBD34. (B, D, F, and H) Single-molecule E_{FRET} trajectories corresponding to the labeling schemes in panels A, C, E, and G, respectively. (I−M) Compiled E_{FRET} distributions for Cy5-Hah1 with $Cy3\text{-}MBD4^{SD}$, Cy5-Hah1 with $Cy3\text{-}MBD34^{L4}$, Cy5-Hah1 with $Cy3\text{-}MBD34^{L3}$, $Cy3Cy5\text{-}MBD34^{L34}$, and $Cy3Cy5\text{-}MBD34^{L34}$ with excess Hah1, respectively. The histograms are Gaussian-resolved; the relative peak areas in each histogram reflect the relative stabilities of corresponding states. Reprinted with permission from refs 94 and 96. Copyright 2008 and 2012, respectively, American Chemical Society.

dx.doi.org/10.1021/bi400597v | Biochemistry 2013, 52, 7170−7183

interactions discussed earlier. Lipid vesicle trapping gives a confined volume, resulting in an approximately micromolar effective protein concentration for a single molecule inside, which is needed for studying weak interactions (micromolar K_D). Vesicle trapping also eliminates nonspecific interactions of protein with glass surfaces while being immobilized and allows us to selectively remove homodimeric interactions between two proteins of the same type during data analysis; these homodimeric interactions inevitably convolute ensemble-averaged measurements and are particularly relevant in studies of Hah1−WDP interactions, as Hah1 (and likely WDP MBDs) can form homodimers in solution.[53,67]

By placing the FRET pair on Hah1, MBD3, and/or MBD4 site-specifically, we systematically studied interactions between Hah1 and the isolated WDP MBD4 (denoted MBD4^{SD}; SD, single domain), between Hah1 and each of the two domains of the double-domain WDP construct MBD34, and between the two MBDs of MBD34 (Figure 8A,C,E,G).[93−96] The labeling positions in Hah1 and each WDP MBD were all at their C-termini of these homologous protein domains. The interactions between Hah1 and MBD4^{SD} provided the foundation for understanding Hah1−WDP interactions, which involve many MBDs. The double-domain construct MBD34 represented the simplest multidomain system, which allowed us to gain insights into the multidomain effect on Hah1−WDP interactions.

Persistent Dynamic Interactions with Two Major Interconverting Complexes Regardless of Metalation State. For all Hah1−MBD and MBD−MBD interactions, we have consistently observed two major interaction complexes that interconvert dynamically, regardless of the protein metalation states. This is best illustrated by Hah1−MBD4^{SD} interactions: the single-molecule E_{FRET} trajectory shows dynamic transitions between the dissociated state (E_{Disso}) and two major complexes (E_{Mid} and E_{High}) (Figure 8B). For interactions of Hah1 with MBD3 or MBD4 within the double-domain construct MBD34, the two higher-E_{FRET} states, E_{Mid} and E_{High}, are preserved (Figure 8D,F); they are also present in MBD3−MBD4 interactions (Figure 8H) (note we use the terms MBD3 and MBD4 to refer to the respective MBDs within the double-domain MBD34 construct). The lowest-E_{FRET} state (i.e., E_{Low}) in the E_{FRET} trajectories of Hah1−MBD3 or Hah1−MBD4 interactions contains the dissociated state (E_{Disso}) and the state (E_{Low}') in which Hah1 interacts with the respective unlabeled MBD of MBD34; these two states overlap significantly but can be resolved in global fitting of the E_{FRET} histograms (Figure 8I−M). E_{Low}' is approximated by the lowest-E_{FRET} state in MBD3−MBD4 interactions (Figure 8H,L), where MBD3 and MBD4 are separated with their peptide linker in an extended conformation.

The conservation of the two major interaction geometries among Hah1−MBD and MBD−MBD interactions is reflected by the similarity of the E_{FRET} values of E_{Mid} and E_{High} (Figure 8I−L). This conservation can be attributed to the homology in sequence and structure across Hah1 and WDP MBDs. One should note that the geometric information from FRET measurements here is limited to the one-dimensional coordinate between the FRET donor and acceptor; three-dimensional geometric information needs multiple labeling schemes that cover multiple directions, which we are currently pursuing.

It is worth noting that earlier NMR studies of interactions between Hah1 and various WDP/MNK constructs did not detect interaction complexes at their apo states,[66,76−82] even though earlier SPR studies did observe apoprotein interactions.[74,75] Our smFRET results represented the first evidence that multiple complexes exist for metallochaperone−target protein interactions regardless of the protein metalation state and further corroborated that Hah1 can form complexes with WDP without Cu^+. Moreover, more recent NMR studies by Fatemi et al. of the interactions between Hah1 and WDP MBD4−6 resolved interactions at their apo states,[83] consistent with our results.

We proposed two structural models for the two observed interaction complexes between Hah1 and WDP MBDs on the basis of our smFRET results and past structural studies of these proteins and other homologues, all of which have the $\beta\alpha\beta\beta\alpha\beta$ fold and contain the CXXC motif. The two α-helices are on one side of the protein (i.e., the "face" side), and the four β-strands form a β-sheet on the other side (i.e., the "back" side). We proposed a face-to-face interaction geometry that gave rise to the E_{Mid} state observed in our smFRET measurements and a face-to-back geometry for the E_{High} state (Figure 9A,B). The

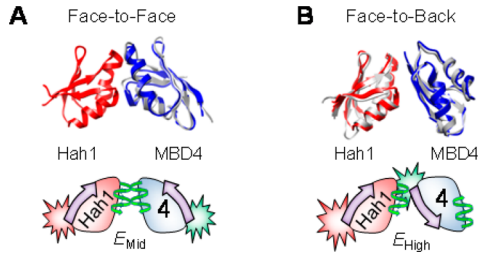

Figure 9. Structural models (top) of face-to-face (A) and face-to-back (B) Hah1−MBD4 interaction complexes with corresponding cartoon representations (bottom). In the cartoons, the face side of a protein is represented by a helix and the back side by an arrow. The FRET label positions are also indicated. Reprinted with permission from ref 96. Copyright 2012 American Chemical Society.

face-to-face geometry has been observed by NMR between Hah1 and MNK1, the first N-terminal MBD of MNK,[82] and in homodimeric complexes of Hah1.[67] The CXXC motifs of the two proteins face each other in this geometry, where Cu^+ can coordinate to cysteines from both proteins, thus offering a facile pathway for copper transfer via ligand exchange.[52,57,59,67−69] The face-to-back geometry was based on the crystal structure of an asymmetric dimer of the MBD of Hma7, a Cu^+-transporting ATPase in *Arabidopsis thaliana*; this MBD is homologous to Hah1 and WDP/MNK MBDs.[85] The FRET donor−acceptor distances in the face-to-face models are longer than those in the face-to-back models, consistent with $E_{Mid} < E_{High}$. The validity of these two models was further supported by detailed interface thermodynamic analysis and molecular dynamics simulations.[96]

Interactions of Hah1 with MBD3 and MBD4 within MBD34 have similar stabilities, reflected by their similar peak areas of the associated states (E_{Mid} and E_{High}) relative to the area of the dissociated state (E_{Disso}) in the E_{FRET} histograms (panel J vs panel K of Figure 8), but the Hah1−MBD4 interactions are significantly more stable than the Hah1−MBD4^{SD} interactions whose peak areas of the E_{Mid} and E_{High} states are much smaller relative to that of the dissociated state (Figure 8I). This enhanced stability in Hah1's interactions with MBD4 within the double-domain construct MBD34 is related to an increase in the rate of protein association, not a decrease in the rate of protein dissociation, because the interaction complexes have

similar lifetimes regardless of whether Hah1 is interacting with MBD4 in MBD34 or with MBD4^{SD}.[96]

In the presence of 1 equiv of Cu^+ (i.e., one protein is in the apo state and the other the holo state), the face-to-face interaction geometry is stabilized significantly for Hah1−MBD4^{SD} interactions, reflected by the increased peak area of the E_{Mid} state relative to that of the E_{Disso} state in E_{FRET} histograms (panel B vs panel A of Figure 10). This stabilization

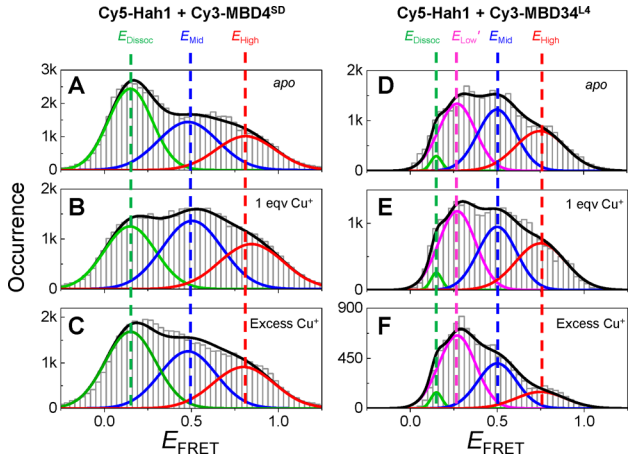

Figure 10. Compiled E_{FRET} distributions for Cy5-Hah1 with Cy3-MBD4^{SD} (A−C) and Cy5-Hah1 with Cy3-MBD34^{L4} (D−F) in the absence and presence of 1 equiv and excess Cu^+ per protein pair. Reprinted with permission from ref 96. Copyright 2012 American Chemical Society. Also reproduced with permission from ref 95. Copyright 2011 The Royal Society of Chemistry.

of the face-to-face geometry at the apo−holo interaction state can be attributed to possible Cu^+ bridging via the CXXC motifs at the protein interaction interface (Figure 9A). Consistently, this stabilization vanishes when both proteins are metalated in the presence of excess Cu^+ (panel C vs panel A of Figure 10). In contrast, this Cu^+ bridging-induced stabilization of the apo−holo interactions in the face-to-face geometry is insignificant for interactions of Hah1 with MBD4 in the double-domain construct MBD34, as no stabilization of the E_{Mid} state was observed in the presence of 1 equiv of Cu^+ (panel E vs panel D of Figure 10). Moreover, under excess Cu^+, the Hah1−MBD4 interactions in both geometries are destabilized relative to those in the absence of Cu^+ (panel F vs panel D of Figure 10), possibly because of a disruption of concerted interactions within the double-domain MBD34, as this destabilization was not observed in Hah1−MBD4^{SD} interactions (panel C vs panel A of Figure 10).

Three-Body Interactions. Quantitative population analysis of different interaction states in different labeling schemes for Hah1−MBD34 interactions also suggested the presence of three-body interactions among Hah1, MBD4, and MBD3. First, an overlap population was observed between Hah1−MBD4 complexes and Hah1−MBD3 complexes, attributed to Hah1 interacting with MBD4 and MBD3 simultaneously. Second, Hah1 can interact with the intramolecular−interdomain MBD3−MBD4 complexes, reflected in part by the population changes in E_{Mid} and E_{High} states in the Cy3Cy5-MBD34^{L34} labeling scheme when an excess of Hah1 was introduced (panel M vs panel L of Figure 8).

In our two proposed interaction geometries, the face and back interfaces are spatially distinct (i.e., nonoverlapping), making possible three-body interactions among Hah1, MBD3, and MBD4. We thus made models for three-body interactions using combinations of face-to-face and face-to-back interactions. Figure 11 illustrates two possible three-body

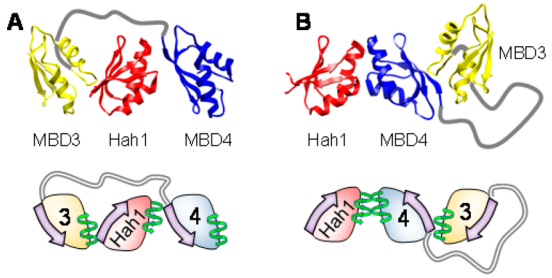

Figure 11. Structural models of three-body interactions in which Hah1 is sandwiched between MBD3 and MBD4 (A) and Hah1 is interacting with an MBD34 intramolecular−interdomain adduct (B). Reprinted with permission from ref 96. Copyright 2012 American Chemical Society.

interactions. In one, Hah1 is sandwiched between MBD3 and MBD4, and in the other, Hah1 interacts with an intramolecular MBD3−MBD4 complex. We should emphasize that the interaction geometries here are only models that are supported by data and deduced from known structures of protein complexes. Within either E_{Mid} or E_{High} states, additional subpopulations could exist that are unresolved in our measurements. The dynamic peptide linker between MBD4 and MBD3 may also play a role in formation of the complex.[89]

Versatile Pathways for Receiving, Redistributing, and Exporting Copper Ions via Multibody Protein Interactions. The ways that Hah1 and the double-domain construct MBD34 can interact suggest versatile pathways for the trafficking of copper from Hah1 to WDP (or MNK) inside cells. This versatility is better illustrated by an analogy to the modern cargo transportation industry. In this analogy, Hah1 is a delivery truck with Cu^+ as its cargo. The N-terminal region of WDP, with multiple MBDs, is a warehouse distribution center, and the MBDs are the loading docks. The distribution center must operate with both efficiency and versatility to receive, reroute, and export shipments from many trucks.

The versatility of operation of the WDP distribution center is accomplished by providing multiple MBD docking sites for the Hah1 truck to deliver its cargo. The truck can park frontward or backward at the dock [i.e., with two major Hah1−MBD interaction geometries (Figure 12A)]. Even better, the truck can interconvert between its docking geometries dynamically, thus allowing either of the two interfaces to be exposed for interaction with an additional MBD. The three-body interactions in which Hah1 is sandwiched between MBDs allow for the rerouting of the delivery truck; i.e., a Hah1 molecule can be handed over directly from one MBD to another (Figure 12D). This rerouting of Hah1 would especially be useful when the initially targeted MBD is already loaded with Cu^+. WDP's intramolecular MBD−MBD interactions provide a method of internal redistribution of the Cu^+ cargo, either to vacate space for the next Hah1 delivery or to transport Cu^+ downstream. This redistribution also occurs in a versatile manner, as two major binding geometries were observed between MBD3 and MBD4 (Figure 12B). This internal cargo redistribution among MBDs can be directly coupled to the cargo delivery or export, through interactions of Hah1 with the

dx.doi.org/10.1021/bi400597v | Biochemistry 2013, 52, 7170−7183

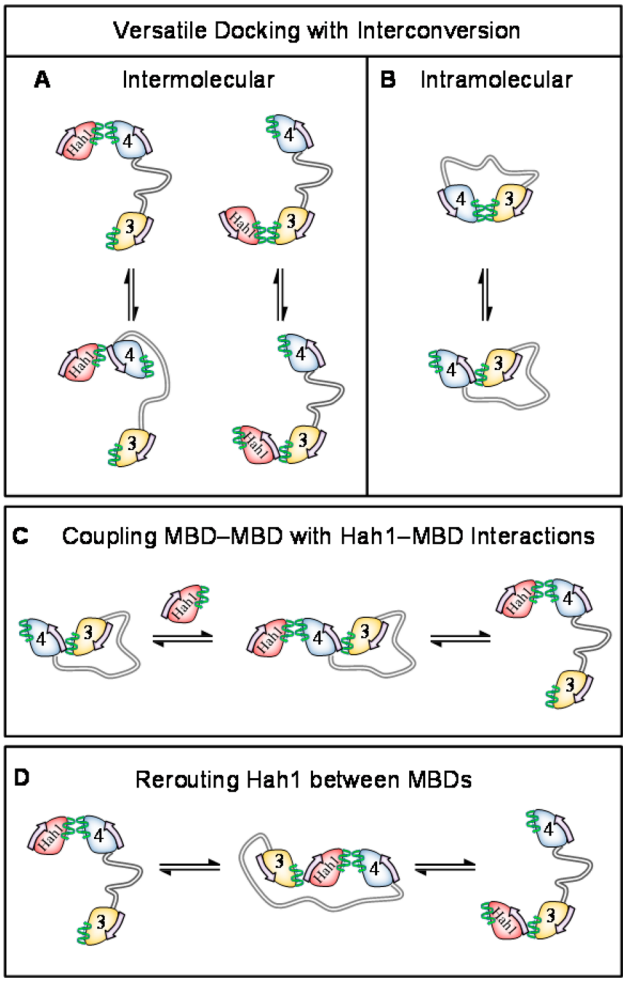

Figure 12. Versatile pathways for the trafficking of copper from Hah1 to WDP MBDs illustrated by the major features of Hah1−MBD34 interaction dynamics. (A and B) Intermolecular and intramolecular Hah1−MBD4, Hah1−MBD3, and MBD3−MBD4 interactions can occur in two major geometries, providing versatile docking with interconversion for Cu^+ transfer. (C) Hah1 can interact with intramolecular−interdomain MBD34 complexes linking MBD−MBD and Hah1−MBD interactions. (D) The three-body interaction in which Hah1 is sandwiched provides a mechanism for rerouting Hah1 between MBDs. Reprinted with permission from ref 96. Copyright 2012 American Chemical Society.

intramolecular MBD−MBD complexes (Figure 12C). All of the interactions described above occur on a time scale of ~1 s,[96] including the protein associations at approximately micromolar concentrations (note the intracellular concentration of the yeast Hah1 homologue Atx1 is also approximately micromolar[97]). Therefore, all these processes should occur comparably inside cells for function.

The ways that Hah1 and MBD34 interact also shed light on the possible regulatory function of the MBDs, in which Hah1−MBD or MBD−MBD interactions modulate the ATPase activity associated with Cu^+ translocation[71,98−101] or the kinase-mediated phosphorylation associated with the relocalization of WDP/MNK for Cu^+ efflux.[71,98−101] It has been proposed that large-scale conformational changes within the N-terminal tail of WDP/MNK can act as a regulatory switch:[80,89,102−105] these changes would disrupt interactions of the MBD with the catalytic core affecting Cu^+ translocation or expose/hide phosphorylation sites in the linker regions. The three-body interactions in which Hah1 is sandwiched between MBDs (Figure 12D) could induce large-scale conformational changes in the cytoplasmic tail of WDP and hence may play a role in this regulatory switching mechanism.

Although our study was limited to Hah1−WDP interactions for Cu^+ trafficking, we suspect that their versatile metal trafficking mechanism may also operate in other P_{IB}-ATPases: many of these ATPases contain multiple MBDs and could have associated metallochaperones, which regulate other metals such as Cd^{2+}, Zn^{2+}, Pb^{2+}, and Ag^+.[72,106]

RELATED SINGLE-MOLECULE BIOINORGANIC WORK

In the past few years, more single-molecule studies of bioinorganic systems have emerged. A few earlier ones were reviewed by us in 2008.[107] Below we briefly summarize these studies according to the techniques employed and refer to relevant reviews for in-depth reviews on these topics. These single-molecule studies provide a context for the single-molecule fluorescence studies our group has pursued. The strengths and limitations of the techniques are also discussed.

Single-Molecule Fluorescence Microscopy Studies. Several groups have used the single-molecule fluorescence quenching strategy to study metalloproteins; this strategy is a variant of FRET in which the acceptor, here a metal-based active site in protein, is a strong chromophore at a certain oxidation state but nonfluorescent and acts as a quencher to an introduced fluorescent label that acts as the donor. Erker, Basché, and co-workers used this strategy to study oxygen binding by binuclear copper protein hemocyanin.[108,109] Aartsman, Canters, Schmidt, and co-workers used this strategy to probe the redox states of blue copper protein azurin.[110,111] Takahashi and co-workers used it to study the folding dynamics of cytochrome *c*.[112] Herten and co-workers used it to monitor the formation and dissociation of metal complexes.[113] Canters, Moerner, and co-workers used it to study the enzymatic reactions by the copper enzyme nitrite reductase.[114,115] Spies and co-workers used it to study the interactions of an iron−sulfur cluster-containing helicase with DNA.[116]

Moreover, Ha, Lu, and co-workers have used smFRET to study the metal ion-dependent folding of DNAzymes. Rigler and co-workers developed the fluorogenic reaction approach to study catalysis by the heme-enzyme horseradish peroxidase,[117,118] in which the fluorescence signal of a reaction product was detected at the single-molecule level to monitor catalytic reactions. The intrinsic fluorescence of Mg^{2+}-containing chlorophyll has also been utilized widely to study light-harvesting complexes at the single-molecule level and has been reviewed elsewhere.[119−126]

Single-molecule fluorescence imaging, including single-molecule FRET and fluorescence quenching discussed here, is broadly applicable for studying protein function and dynamics. The use of external fluorescent probes is general. Site-specific labeling of proteins is readily achievable with many accessible labeling schemes, including site-directed mutagenesis, GFP fusion, and unnatural amino acids.[127,128] Many fluorescent probes suitable for singe-molecule detections are also available covering a wide spectral range.[128] The single-molecule fluorescence quenching strategy has particular potential for studying metalloproteins; in principle, any metalloprotein that shows intense absorption properties can be targeted using this approach. Moreover, transition metal-based chemistry often involves species that have intense ligand-to-metal charge

transfer absorptions. These strong chromophoric species can be exploited as quenching centers for single-molecule fluorescence detection.

Limitations to fluorescence-based single-molecule methods also exist. For example, photobleaching of the probe limits the observation time window. With a good oxygen scavenging system, a single fluorescent probe molecule can last for up to a few minutes before being photobleached.[129] The introduction of fluorescent probes always bring concerns of perturbation to protein structure and function, for which careful controls need to be conducted to ensure that the perturbation is not significant.

Single-Molecule Scanning Probe Microscopy Studies. Scanning probe microscopies have also been applied in studying metalloproteins at the single-molecule level. These studies are approximately in two categories: scanning tunneling microscopy (STM) and atomic force microscopy (AFM). STM was used to study the electron transfer properties of single metalloproteins via electrical current measurements. The STM studies by Ulstrup,[130,131] Facci,[132] and co-workers on electron transfer by metalloproteins and by Cannistraro[133] and co-workers on electron conduction and recognition by metalloproteins have been reviewed by these researchers. Winggington,[134] Jones,[135] and co-workers have used STM to measure tunneling currents through single cytochrome molecules. AFM was used to manipulate metalloproteins mechanically (i.e., by force). Cannistraro and co-workers used single-molecule force measurements to study the recognition between cytochrome c_{551} and azurin[136,137] and the interaction between p53 and azurin.[138,139] Yersin,[140] Ikuta,[141] and co-workers studied transferrin−receptor interactions. Li and co-workers studied the metal−thiolate bond ruptures in rubredoxin.[142,143]

The electric current-based detection of scanning probe microscopy (e.g., STM) is powerful for interrogating the electron transfer properties of redox-active proteins, many of which contain a redox-active metal center. The measurements can also be performed for an extended time on a single protein molecule, allowing the study of time-dependent behaviors. The mechanics-based approach (e.g., AFM) measures force directly, which readily connects to thermodynamic properties, such as the interaction affinity between proteins. The scanning probe can also be used to manipulate protein molecules, offering a way to control and change protein structure or function.

Limitations to these approaches also exist. The current-based detection is limited to redox-active proteins. Many redox-inactive metalloproteins, such as Zn^{II}-containing ones, are thus not accessible. The mechanics-based detection is based on measuring force or distance changes; processes that do not cause force or distance changes, for example, most enzymatic reactions, would be challenging to study. The scanning probe approach is a serial measurement, in which only one molecule is studied at a time, leading to low data throughput.

■ CONCLUDING REMARKS

The reach of single-molecule studies has been expanding rapidly in recent years, not only in biological sciences but also in physical sciences (e.g., in heterogeneous catalysis[144]). Single-molecule research in the bioinorganic field is still underpopulated. Vast opportunities exist for new research endeavors. Of particular interest to us, the advances in the cell biology of metals continue to unravel new scientific problems. We are currently continuing our studies of metalloregulators and metallochaperones, with more focus on living cell studies at the single-molecule level. Studying how these metalloproteins operate *in vivo* is important, as a cell presents a much more complicated environment than a test tube, such as compartmentation, localization, crowdedness, and nonspecific interactions, which *in vitro* experimental conditions may not capture. The mechanism of a metal homeostatic protein, or any protein, can be significantly affected by its cellular spatiotemporal state, i.e., where it is in the cell and when. To obtain such information, one needs to interrogate protein functions in a living cell in a spatiotemporally resolved manner. For bacteria, which are merely a few micrometers in size, this interrogation requires nanometer spatial resolution, beyond the reach of conventional optical microscopy (at best ∼250 nm resolution), while electron microscopy or scanning probe microscopy, with their nanometer resolution, cannot probe into living cells. For eukaryotic cells, many of their internal compartments, such as organelles, are also small in size and require nanometer spatial resolution to resolve. High sensitivity is often needed, too, especially for low-copy number proteins (e.g., metalloregulators, which are transcription factors). Single-molecule fluorescence imaging techniques can meet many of these requirements, for example, nanometer resolution (via a super-resolution imaging approach based on single-molecule detection[144−147]), single-molecule sensitivity, millisecond temporal resolution, and high specificity in imaging cellular processes (e.g., through genetically tagging with fluorescent proteins). It is the authors' belief that the application of single-molecule imaging could create a new subarea in bioinorganic research, breaking new ground and establishing new directions. The opportunities are limited only by one's imagination.

■ AUTHOR INFORMATION

Corresponding Author

*E-mail: pc252@cornell.edu. Phone: (607) 254-8533.

Present Addresses

[†]A.M.K.: Center for Integrated Nanotechnologies, Los Alamos National Laboratory, Los Alamos, NM 87545.

[‡]N.M.A.: Department of Cell Biology, Harvard Medical School, Boston, MA 02115.

[§]J.J.B.: School of Applied and Engineering Physics, Cornell University, Ithaca, NY 14853.

Funding

We thank the National Institutes of Health (GM082939, GM106420, and EB009202), the National Science Foundation (CHE-0645392), and Optofluidics Inc. for financial support.

Notes

The authors declare no competing financial interest.

■ ACKNOWLEDGMENTS

We thank Debashis Panda, Derek Klarin, and Matthew Goldfogel for their contributions and David Erickson, Peng R. Chen and Chuan He, Ahmed Gaballa and John Helmann, David Huffman, Liliya Yatsunyk and Amy Rosenzweig, and Linghao Zhong for collaborations on the research reviewed here.

■ ABBREVIATIONS

CueR, copper efflux regulator; MerR, mercury resistance regulator; CopA, copper-exporting ATPase; CueO, copper efflux oxidase; RNAp, RNA polymerase; smFRET, single-molecule fluorescence resonance energy transfer; HJ, Holliday junction; MerD, mercury resistance coregulator; Hah1, human

Atx1 homologue; Atox1, antioxidant protein 1; WDP, Wilson's disease protein; MNK, Menkes disease protein; MBD, metal-binding domain.

■ ADDITIONAL NOTE

[a]On the potential energy surface going from the reactant to the product along the reaction coordinate, a transition state is a first-order saddle point, where there is a minimum in all dimensions but one. On the other hand, an intermediate is a local minimum in all dimensions.

■ REFERENCES

(1) Lippard, S. J., and Berg, J. M. (1994) *Principles of Bioinorganic Chemistry*, University Science Books, Mill Valley, CA.

(2) Holm, R. H., and Solomon, E. I., Eds. (1996) Thematic Issue: Bioinorganic Enzymology. *Chemical Reviews*, Vol. *96*, Issue 7, American Chemical Society, Washington, DC.

(3) Michalet, X., Weiss, S., and Jaeger, M. (2006) Single-molecule fluorescence studies of protein folding and conformational dynamics. *Chem. Rev. 106*, 1785−1813.

(4) Zhuang, X. (2005) Single-Molecule RNA Science. *Annu. Rev. Biophys. Biomol. Struct. 34*, 399−414.

(5) Selvin, P. R., and Ha, T., Eds. (2008) *Single Molecule Techniques: A Laboratory Manual*, Cold Spring Harbor Laboratory Press, Plainview, NY.

(6) Smiley, R. D., and Hammes, G. G. (2006) Single Molecule Studies of Enzyme Mechanisms. *Chem. Rev. 106*, 3080−3094.

(7) Xie, X. S., Choi, P. J., Li, G.-W., Lee, N. K., and Lia, G. (2008) Single-Molecule Approach to Molecular Biology in Living Bacterial Cells. *Annu. Rev. Biophys. 37*, 417−444.

(8) Bustamante, C., Macosko, J. C., and Wuite, G. J. L. (2000) Grabbing the cat by the tail: Manipulating molecules one by one. *Nat. Rev. Mol. Cell Biol. 1*, 130−136.

(9) Chen, P., Andoy, N. M., Benitez, J. J., Keller, A. M., Panda, D., and Gao, F. (2010) Tackling Metal Regulation and Transport at the Single-Molecule Level. *Nat. Prod. Rep. 27*, 757−767.

(10) O'Halloran, T. V. (1993) Transition Metals in Control of Gene Expression. *Science 261*, 715−725.

(11) Giedroc, D. P., and Arunkumar, A. I. (2007) Metal Sensor Proteins: Nature's Metalloregulated Allosteric Switch. *Dalton Trans.*, 3107−3120.

(12) Waldron, K. J., Rutherford, J. C., Ford, D., and Robinson, N. J. (2009) Metalloproteins and Metal Sensing. *Nature 460*, 823−830.

(13) Barkey, T., Miler, S. M., and Summers, A. O. (2003) Bacterial Mercury Resistance from Atoms to Ecosystems. *FEMS Microbiol. Rev. 27*, 355−384.

(14) Brown, N. L., Stoyanov, J. V., Kidd, S. P., and Hobman, J. L. (2003) The MerR Family of Transcripitional Regulators. *FEMS Microbiol. Rev. 27*, 145−163.

(15) Busenlehner, L., Pennella, M. A., and Giedroc, D. P. (2003) The SmtB/ArsR Family of Metalloregulatory Transcriptional Repressors: Structural Insights into Prokaryotic Metal Resistance. *FEMS Microbiol. Rev. 27*, 131−143.

(16) Andrews, S. C., Robinson, A. K., and Rodriguez-Quinones, F. (2003) Bacterial Iron Homeostasis. *FEMS Microbiol. Rev. 27*, 215−237.

(17) Cavet, J. S., Borrelly, G. P. M., and Robinson, N. J. (2003) Zn, Cu and Co in Cyanobacteria: Selective Control of Metal Availability. *FEMS Microbiol. Rev. 27*, 165−181.

(18) Mergeay, M., Monchy, S., Vallaeys, T., Auquier, V., Benotmane, A., Bertin, P., Taghavi, S., Dunn, J., van der Lelie, D., and Wattiez, R. (2003) *Ralstonia metallidurans*, a Bacterium Specifically Adapted to Toxic Metals: Towards a Catalogue of Metal-Reponsive Genes. *FEMS Microbiol. Rev. 27*, 385−410.

(19) Rensing, C., and Grass, G. (2003) *Escherichia coli* Mechanisms of Copper Homeostasis in a Changing Environment. *FEMS Microbiol. Rev. 27*, 197−213.

(20) Solioz, M., and Stoyanov, J. V. (2003) Copper Homeostasis in *Enterococcus hirae*. *FEMS Microbiol. Rev. 27*, 183−195.

(21) Kehres, D. G., and Maguire, M. E. (2003) Emerging Themes in Manganese Transport, Biochemistry and Pathogenesis in Bacteria. *FEMS Microbiol. Rev. 27*, 263−290.

(22) Lloyd, J. R. (2003) Microbial Reduction of Metals and Radionuclides. *FEMS Microbiol. Rev. 27*, 411−425.

(23) Mulrooney, S. B., and Hausinger, R. P. (2003) Nickel Uptake and Utilization by Microorganism. *FEMS Microbiol. Rev. 27*, 239−261.

(24) Nies, D. H. (2003) Efflux-Mediated Heavy Meal Resistance in Prokaryotes. *FEMS Microbiol. Rev. 27*, 313−339.

(25) Hobman, J. L., Wilkie, J., and Brown, N. L. (2005) A Design for Life: Prokaryotic Metal-Bindng MerR Family Regulators. *BioMetals 18*, 429−436.

(26) Laity, J. H., and Andrews, G. K. (2007) Understanding the mechanisms of zinc-sensing by metal-response element binding transcription factor-1 (MTF-1). *Arch. Biochem. Biophys. 463*, 201−210.

(27) O'Halloran, T. V., Frantz, B., Shin, M. K., Ralston, D. M., and Wright, J. G. (1989) The MerR Heavy Metal Receptor Mediates Positive Activation in a Topologically Novel Transcription Complex. *Cell 56*, 119−129.

(28) Frantz, B., and O'Halloran, T. V. (1990) DNA Distortion Accompanies Transcriptional Activation by the Metal-Responsive Gene-Regulatory Protein MerR. *Biochemistry 29*, 4747−4751.

(29) Chen, P. R., and He, C. (2008) Selective recognition of metal ions by metalloregulatory proteins. *Curr. Opin. Chem. Biol. 12*, 214−221.

(30) Newberry, K. J., and Brennan, R. G. (2004) The Structural Mechanism for Transcription Activation by MerR Family Member Multidrug Transporter Activation, N-Terminus. *J. Biol. Chem. 279*, 20356−20362.

(31) Outten, C. E., Outten, F. W., and O'Halloran, T. V. (1999) DNA Distortion Mechanism for Transcriptional Activation by ZntR, a Zn(II)-responsive MerR Homologue in *Escherichia coli*. *J. Biol. Chem. 274*, 37517−37524.

(32) Holm, R. H., Kennepohl, P., and Solomon, E. I. (1996) Structural and Functional Aspects of Metal Sites in Biology. *Chem. Rev. 96*, 2239−2314.

(33) Changela, A., Chen, K., Xue, Y., Holschen, J., Outten, C. E., O'Halloran, T. V., and Mondragon, A. (2003) Molecular Basis of Metal-Ion Selectivity and Zeptomolar Sensitivity by CueR. *Science 301*, 1383−1387.

(34) Rosenzweig, A. C., and O'Halloran, T. V. (2000) Structure and Chemistry of the Copper Chaperone Proteins. *Curr. Opin. Chem. Biol. 4*, 140−147.

(35) Joshi, C. P., Panda, D., Martell, D. J., Andoy, N. M., Chen, T.-Y., Gaballa, A., Helmann, J. D., and Chen, P. (2012) Single-Molecule Analysis Suggests Novel Pathways for Turning Off Transcription by a MerR-family Metalloregulator. *Proc. Natl. Acad. Sci. U.S.A. 109*, 15121−15126.

(36) Outten, F. W., Outten, C. E., Hale, J., and O'Halloran, T. V. (2000) Transcriptional Activation of an *Escherichia coli* Copper Efflux Regulation by the Chromosomal MerR Homologue, CueR. *J. Biol. Chem. 275*, 31024−31029.

(37) Stoyanov, J. V., Hobman, J. L., and Brown, N. L. (2001) CueR (YbbI) of *Escherichia coli* Is a MerR Family Regulator Controlling Expression of the Copper Exporter CopA. *Mol. Microbiol. 39*, 502−511.

(38) Outten, F. W., Huffman, D. L., Hale, J. A., and O'Halloran, T. V. (2001) The Independent *cue* and *cus* Systems Confer Copper Tolerance during Aerobic and Anaerobic Growth in *Escherichia coli*. *J. Biol. Chem. 2001*, 30670−30677.

(39) Grass, G., and Rensing, C. (2001) Genes Involved in Copper Homeostasis in *Escherichia coli*. *J. Bacteriol. 133*, 2145−2147.

(40) Abbondanzieri, E. A., Bokinsky, G., Rausch, J. W., Zhang, J. X., Le Grice, S. F. J., and Zhuang, X. (2008) Dynamic binding orientations direct activity of HIV reverse transcriptase. *Nature 453*, 184−189.

(41) Blattner, F. R., Plunkett, G., Bloch, C. A., Perna, N. T., Burland, V., Riley, M., Collado-Vides, J., Glasner, J. D., Rode, C. K., Mayhew, G.

F., Gregor, J., Davis, N. W., Kirkpatrick, H. A., Goeden, M. A., Rose, D. J., Mau, B., and Shao, Y. (1997) The Complete Genome Sequence of *Escherichia coli* K-12. *Science 277*, 1453−1462.
(42) von Hippel, P. H., and Berg, O. G. (1989) Facilitated target location in biological systems. *J. Biol. Chem. 264*, 675−678.
(43) Blainey, P. C., Graziano, V., Pérez-Berná, A. J., McGrath, W. J., Flint, S. J., Martín, C. S., Xie, X. S., and Mange, W. F. (2013) Regulation of a Viral Proteinase by a Peptide and DNA in One-dimensional Space: IV. Viral Proteinase Slides along DNA To Locate and Process Its Substrates. *J. Biol. Chem. 288*, 2092−2102.
(44) Graham, J. S., Johnson, R. C., and Marko, J. F. (2011) Concentration-dependent exchange accelerates turnover of proteins bound to double-stranded DNA. *Nucleic Acids Res. 39*, 2249−2259.
(45) Andoy, N. M., Sarkar, S. K., Wang, Q., Panda, D., Benitez, J. J., Kalininskiy, A., and Chen, P. (2009) Single-Molecule Study of Metalloregulator CueR-DNA Interactions Using Engineered Holliday Junctions. *Biophys. J. 97*, 844−852.
(46) Eichman, B. F., Vargason, J. M., Mooers, B. H. M., and Ho, P. S. (2000) The Holliday junction in an inverted repeat DNA sequence: Sequence effects on the structure of four-way junctions. *Proc. Natl. Acad. Sci. U.S.A. 97*, 3971−3976.
(47) Ortiz-Lombardía, M., González, A., Eritja, R., Aymamí, J., Azorín, F., and Coll, M. (1999) Crystal structure of a DNA Holliday junction. *Nat. Struct. Biol. 6*, 913−917.
(48) McKinney, S. A., Declais, A. C., Lilley, D. M. J., and Ha, T. (2003) Structural Dynamics of Individual Holliday Junctions. *Nat. Struct. Biol. 10*, 93−97.
(49) Sarkar, S. K., Andoy, N. M., Benitez, J. J., Chen, P. R., Kong, J. S., He, C., and Chen, P. (2007) Engineered Holliday Junctions as Single-Molecule Reporters for Protein-DNA Interactions with Application to a MerR-Family Regulator. *J. Am. Chem. Soc. 129*, 12461−12467.
(50) Karymov, M. A., Chinnaraj, M., Bogdanov, A., Srinivasan, A. R., Zheng, G., Olson, W. K., and Lyubchenko, Y. L. (2008) Structure, dynamics, and branch migration of a DNA Holliday junction: A single-molecule fluorescence and modeling study. *Biophys. J. 95*, 4372−4383.
(51) Yamamoto, K., and Ishihama, A. (2004) Transcriptional Response of *Escherichia coli* to External Copper. *Mol. Microbiol. 56*, 215−227.
(52) O'Halloran, T. V., and Culotta, V. C. (2000) Metallochaperones, an Intracellular Shuttle Service for Metal Ions. *J. Biol. Chem. 275*, 25057−25060.
(53) Rosenzweig, A. C. (2001) Copper Delivery by Metallochaperone Proteins. *Acc. Chem. Res. 34*, 119−128.
(54) Donnelly, P. S., Xiao, Z., and Wedd, A. G. (2007) Copper and Alzheimer's disease. *Curr. Opin. Chem. Biol. 11*, 128−133.
(55) Cobine, P. A., Pierrel, F., and Winge, D. R. (2006) Copper trafficking to the mitochondrion and assembly of copper metalloenzymes. *Biochim. Biophys. Acta 1763*, 759−772.
(56) Subramanian, P., Rodrigues, A. V., Ghimire-Rijal, S., and Stemmler, T. L. (2011) Iron chaperones for mitochondrial Fe-S cluster biosynthesis and ferritin iron storage. *Curr. Opin. Chem. Biol. 15*, 312−318.
(57) Pufahl, R. A., Singer, C. P., Peariso, K. L., Lin, S.-J., Schmidt, P. J., Fahrni, C. J., Culotta, V. C., Penner-Hahn, J. E., and O'Halloran, T. V. (1997) Metal Ion Chaperone Function of the Soluble Cu(I) Receptor Atx1. *Science 278*, 853−856.
(58) Hamza, I., Schaefer, M., Klomp, L. W. J., and Gitlin, J. D. (1999) Interaction of the Copper Chaperone Hah1 with the Wilson Disease Protein Is Essential for Copper Homeostasis. *Proc. Natl. Acad. Sci. U.S.A. 96*, 13363−13368.
(59) Larin, D., Mekios, C., Das, K., Ross, B., Yang, A.-S., and Gilliam, T. C. (1999) Characterization of the Interaction between the Wilson and Menkes Disease Proteins and the Cytoplasmic Copper Chaperone, Hah1p. *J. Biol. Chem. 274*, 28497−28504.
(60) Boal, A. K., and Rosenzweig, A. C. (2009) Structural Biology of Copper Trafficking. *Chem. Rev. 109*, 4760−4779.
(61) Yatsunyk, L. A., and Rosenzweig, A. C. (2007) Copper(I) Binding and Transfer by the N-terminus of the Wilson Disease Protein. *J. Biol. Chem. 282*, 8622−8631.
(62) Xiao, Z., Brose, J., Schimo, S., Ackland, S. M., La Fontaine, S., and Wedd, A. G. (2011) Unification of the copper(I) binding affinities of the metallo-chaperones Atx1, Atox1, and related proteins: Detection probes and affinity standards. *J. Biol. Chem. 286*, 11047−11055.
(63) Banci, L., Bertini, I., Ciofi-Baffoni, S., Kozyreva, T., Zovo, K., and Palumaa, P. (2010) Affinity gradients drive copper to cellular destinations. *Nature 465*, 645−648.
(64) Badarau, A., and Dennison, C. (2011) Copper trafficking mechanism of CXXC-containing domains: Insight from the pH-dependence of their Cu(I) affinities. *J. Am. Chem. Soc. 133*, 2983−2988.
(65) Xiao, Z., and Wedd, A. G. (2010) The challenges of determining metal-protein affinities. *Nat. Prod. Rep. 27*, 768−789.
(66) Banci, L., Bertini, I., Cantini, F., Massagni, C., Migliardi, M., and Rosato, A. (2009) An NMR Study of the Interaction of N-terminal Cytoplasmic Tail of the Wilson Disease Protein with Copper(I)-Hah1. *J. Biol. Chem. 284*, 9354−9360.
(67) Wernimont, A. K., Huffman, D. L., Lamb, A. L., O'Halloran, T. V., and Rosenzweig, A. C. (2000) Structural Basis for Copper Transfer by the Metallochaperone for the Menkes/Wilson Disease Proteins. *Nat. Struct. Biol. 7*, 766−771.
(68) Arnesano, F., Banci, L., Bertini, I., and Bonvin, M. J. J. (2004) A Docking Approach to the Study of Copper Trafficking Proteins: Interactions between Metallochaperones and Soluble Domains of Copper ATPases. *Structure 12*, 669−676.
(69) Huffman, D. L., and O'Halloran, T. V. (2001) Function, Structure, and Mechanism of Intracellular Copper Trafficking Proteins. *Annu. Rev. Biochem. 70*, 677−701.
(70) Rodriguez-Granillo, A., Crespo, A., Estrin, D. A., and Wittung-Stafshede, P. (2010) Copper-Transfer Mechanism from the Human Chaperone Atox1 to a Metal-Binding Domain of Wilson Disease Protein. *J. Phys. Chem. B 114*, 3698−3706.
(71) Arguello, J. M., Eren, E., and Gonzalez-Guerrero, M. (2007) The structure and function of heavy metal transport P1B-ATPases. *BioMetals 20*, 233−248.
(72) Arguello, J. M. (2003) Identification of ion-selectivity determinants in heavy-metal transport P1B-type ATPases. *J. Membr. Biol. 195*, 93−108.
(73) Huffman, D. L., and O'Halloran, T. V. (2000) Energetics of Copper Trafficking between the Atx1 Metallochaperone and the Intracellular Copper Transporter Ccc2. *J. Biol. Chem. 275*, 18611−18614.
(74) Multhaup, G., Strausak, D., Bissig, K.-D., and Solioz, M. (2001) Interaction of the CopZ Copper Chaperone with the CopA Copper ATPase of *Enterococcus hirae* Assessed by Surface Plasmon Resonance. *Biochem. Biophys. Res. Commun. 288*, 172−177.
(75) Strausak, D., Howies, M. K., Firth, S. D., Schlicksupp, A., Pipkorn, R., Multhaup, G., and Mercer, J. F. B. (2003) Kinetic Analysis of the Interaction of the Copper Chaperone Atox1 with the Metal Binding Sites of the Menkes Protein. *J. Biol. Chem. 278*, 20821−20827.
(76) Arnesano, F., Banci, L., Bertini, I., Cantini, F., Ciofi-Baffoni, S., Huffman, D. L., and O'Halloran, T. V. (2001) Characterization of the Binding Interfaces between the Copper Chaperone Atx1 and the First Cytosolic Domain of Ccc2 ATPase. *J. Biol. Chem. 276*, 41365−41376.
(77) Banci, L., Bertini, I., Cantini, F., Felli, I. C., Gonnelli, L., Hadjiliadis, N., Pierattelli, R., Rosato, A., and Voulgaris, P. (2006) The Atx1-Ccc2 Complex is a Metal-Mediated Protein-Protein Interaction. *Nat. Chem. Biol. 2*, 367−368.
(78) Banci, L., Bertini, I., Cantini, F., Chasapis, C. T., Hadjiliadis, N., and Rosato, A. (2005) A NMR Study of the Interactions of a Three-Domain Construct of ATP7A with Copper(I) and Copper(I)-Hah1: The Interplay of Domains. *J. Biol. Chem. 280*, 38259−38263.
(79) Achila, D., Banci, L., Bertini, I., Bunce, J., Ciofi-Baffoni, S., and Huffman, D. L. (2006) Structure of human Wilson protein domains 5 and 6 and their interplay with domain 4 and the copper chaperone HAH1 in copper uptake. *Proc. Natl. Acad. Sci. U.S.A. 103*, 5729−5734.

(80) Banci, L., Bertini, I., Cantini, F., Della-Malva, N., Migliardi, M., and Rosato, A. (2007) The Different Intermolecular Interactions of the Soluble Copper-Binding Domains of the Menkes Protein, ATP7A. *J. Biol. Chem. 282*, 23140−23146.
(81) Banci, L., Bertini, I., Francesca, C., Rosenzweig, A. C., and Yatsunyk, L. A. (2008) Metal Binding Domains 3 and 4 of the Wilson Disease Protein: Solution Structure and Interaction with the Copper(I) Chaperone Hah1. *Biochemistry 47*, 7423−7429.
(82) Banci, L., Bertini, I., Calderone, V., Della-Malva, N., Felli, I. C., Neri, S., Pavelkova, A., and Rosato, A. (2009) Copper(I)-mediated protein-protein interactions result from suboptimal interaction surfaces. *Biochem. J. 422*, 37−42.
(83) Fatemi, N., Korzhnev, D. M., Velyvis, A., Sarkar, B., and Forman-Kay, J. D. (2010) NMR Characterization of Copper-Binding Domains 4−6 of ATP7B. *Biochemistry 49*, 8468−8477.
(84) Badarau, A., Firbank, S. J., McCarthy, A. A., Banfield, M. J., and Dennison, C. (2010) Visualizing the Metal-Binding Versatility of Copper Trafficking Sites. *Biochemistry 49*, 7798−7810.
(85) Zimmerman, M., Clarke, O., Gulbis, J. M., Keizer, D. W., Jarvis, R. S., Cobbett, C. S., Hinds, M. G., Xiao, Z., and Wedd, A. G. (2009) Metal Binding Affinities of *Arabidopsis* Zinc and Copper Transporters: Selectivities Match the Relative, but Not the Absolute, Affinities of their Amino-Terminal Domains. *Biochemistry 48*, 11640−11654.
(86) Alvarez, H. M., Xue, Y., Robinson, C. D., Canalizo-Hernández, M. A., Marvin, R. G., Kelly, R. A., Mondragón, A., Penner-Hahn, J. E., and O'Halloran, T. V. (2009) Tetrathiomolybdate Inhibits Copper Trafficking Proteins Through Metal Cluster Formation. *Science 327*, 331−334.
(87) Rodriguez-Granillo, A., Crespo, A., and Wittung-Stafshede, P. (2009) Conformational Dynamics of Metal-Binding Domains in Wilson Disease Protein: Molecular Insights into Selective Copper Transfer. *Biochemistry 48*, 5849−5863.
(88) Hussain, F., Rodriguez-Granillo, A., and Wittung-Stafshede, P. (2009) Lysine-60 in Copper Chaperone Atox1 Plays an Essential Role in Adduct Formation with a Target Wilson Disease Domain. *J. Am. Chem. Soc. 131*, 16371−16373.
(89) Rodriguez-Granillo, A., Crespo, A., and Wittung-Stafshede, P. (2010) Interdomain interactions modulate collective dynamics of the metal-binding domains in the Wilson disease protein. *J. Phys. Chem. B 114*, 1836−1848.
(90) Chiu, D. T., Wilson, C. F., Karlsson, A., Danielsson, A., Lundqvist, A., Strömberg, A., Ryttsén, F., Davidson, M., Nordholm, S., Orwar, O., and Zare, R. N. (1999) Manipulating the biochemical nanoenvironment around single molecules contained within vesicles. *Chem. Phys. 247*, 133−139.
(91) Boukobza, E., Sonnenfeld, A., and Haran, G. (2001) Immobilization in Surface-Tethered Lipid Vesicles as a New Tool for Single Biomolecule Spectroscopy. *J. Phys. Chem. B 105*, 12165−12170.
(92) Okumus, B., Wilson, T. J., Lilley, D. M. J., and Ha, T. (2004) Vesicle Encapsulation Studies Reveal that Single Molecule Ribozyme Heterogeneities Are Intrinsic. *Biophys. J. 87*, 2798−2806.
(93) Benitez, J. J., Keller, A. M., and Chen, P. (2010) Nanovesicle Trapping for Studying Weak Protein Interactions by Single-Molecule FRET. *Methods Enzymol. 472*, 41−60.
(94) Benitez, J. J., Keller, A. M., Ochieng, P., Yatsunyk, L. A., Huffman, D. L., Rosenzweig, A. C., and Chen, P. (2008) Probing Real-time Transient Metallochaperone-Target Protein Interactions at the Single-Molecule Level with Nanovesicle Trapping. *J. Am. Chem. Soc. 130*, 2446−2447.
(95) Benitez, J. J., Keller, A. M., Huffman, D. L., Yatsunyk, L., Rosenzweig, A. C., and Chen, P. (2011) Relating Dynamic Protein Interactions of Metallochaperones with Metal Transfer at the Single-Molecule Level. *Faraday Discuss. 148*, 71−82.
(96) Keller, A. M., Benitez, J. J., Klarin, D., Zhong, L., Goldfogel, M., Yang, F., Chen, T.-Y., and Chen, P. (2012) Dynamic Multi-Body Protein Interactions Suggest Versatile Pathways for Copper Trafficking. *J. Am. Chem. Soc. 134*, 8934−8943.
(97) Portnoy, M. E., Rosenzweig, A. C., Rae, T. D., Huffman, D. L., O'Halloran, T. V., and Culotta, V. C. (1999) Structure-Function Analyses of the ATX1 Metallochaperone. *J. Biol. Chem. 274*, 15041−15045.
(98) Lutsenko, S., LeShane, E. S., and Shinde, U. (2007) Biochemical Basis of Regulation of Human Copper-Transporting ATPase. *Arch. Biochem. Biophys. 463*, 134−148.
(99) Gonzalez-Guerrero, M., and Arguello, J. M. (2008) Mechanism of Cu^+-transporting ATPases: Soluble Cu^+ chaperones directly transfer Cu^+ to transmembrane transport sites. *Proc. Natl. Acad. Sci. U.S.A. 105*, 5992−5997.
(100) Wu, C. C., Rice, W. J., and Stokes, D. L. (2008) Structure of a copper pump suggests a regulatory role for its metal-binding domain. *Structure 16*, 976−985.
(101) Gourdon, P., Liu, X. Y., Skjorringe, T., Morth, J. P., Moller, L. B., Pedersen, B. P., and Nissen, P. (2011) Crystal structure of a copper-transporting PIB-type ATPase. *Nature 475*, 59−64.
(102) Leshane, E. S., Shinde, U., Walker, J. M., Barry, A. N., Blackburn, N. J., Ralle, M., and Lutsenko, S. (2010) Interactions between copper-binding sites determine the redox status and conformation of the regulatory N-terminal domain of ATP7B. *J. Biol. Chem. 285*, 6327−6336.
(103) Tsivkovskii, R., MacArthur, B. C., and Lutsenko, S. (2001) The Lys1010-Lys1325 fragment of the Wilson's disease protein binds nucleotides and interacts with the N-terminal domain of this protein in a copper-dependent manner. *J. Biol. Chem. 276*, 2234−2242.
(104) DiDonato, M., Hsu, H. F., Narindrasorasak, S., Que, L., Jr., and Sarkar, B. (2000) Copper-induced conformational changes in the N-terminal domain of the Wilson disease copper-transporting ATPase. *Biochemistry 39*, 1890−1896.
(105) Walker, J. M., Huster, D., Ralle, M., Morgan, C. T., Blackburn, N. J., and Lutsenko, S. (2004) The N-Terminal Metal-Binding Site 2 of the Wilson's Disease Protein Play a Key Role in the Transfer of Copper from Atox1. *J. Biol. Chem. 279*, 15376−15384.
(106) Rosenzweig, A. C., and Argüello, J. M. (2012) Toward a Molecular Understanding of Metal Transport by P_{1B}-Type ATPases. *Curr. Top. Membr. 69*, 113−136.
(107) Chen, P., and Andoy, N. M. (2008) Single-Molecule Fluorescence Studies from a Bioinorganic Perspective. *Inorg. Chim. Acta 361*, 809−819.
(108) Erker, W., Lippitz, M., Basche, T., and Decker, H. (2004) Toward oxygen binding curves of single respiratory proteins. *Micron 35*, 111−113.
(109) Erker, W., Sdorra, S., and Basche, T. (2005) Detection of Single Oxygen Molecules with Fluorescence-Labeled Hemocyanins. *J. Am. Chem. Soc. 127*, 14532−14533.
(110) Schmauder, R., Librizzi, F., Canters, G. W., Schmidt, T., and Aartsma, T. J. (2005) The Oxidation State of a Protein Observed Molecule-by-Molecule. *ChemPhysChem 6*, 1381−1386.
(111) Elmalk, A. T., Salverda, J. M., Tabares, L. C., Canters, G. W., and Aartsma, T. J. (2012) Probing redox proteins on a gold surface by single molecule fluorescence spectroscopy. *J. Chem. Phys. 136*, 235101.
(112) Kinoshita, M., Kamagata, K., Maeda, A., Goto, Y., Komatsuzaki, T., and Takahashi, S. (2007) Development of a technique for the investigation of folding dynamics of single proteins for extended time periods. *Proc. Natl. Acad. Sci. U.S.A. 104*, 10453−10458.
(113) Kiel, A., Kovacs, J., Mokhir, A., Krämer, R., and Herten, D. P. (2007) Direct monitoring of formation and dissociation of individual metal complexes by single-molecule fluorescence spectroscopy. *Angew. Chem., Int. Ed. 46*, 3363−3366.
(114) Kuznetsova, S., Zauner, G., Aartsma, T., Engelkamp, H., Hatzakis, N., Rowan, A. E., Nolte, R. J. M., Christianen, P. C. M., and Canters, G. W. (2008) The Enzyme Mechanism of Nitrite Reductase Studied at Single-Molecule Level. *Proc. Natl. Acad. Sci. U.S.A. 105*, 3250−3255.
(115) Goldsmith, R. H., Tabares, L. C., Kostrz, D., Dennison, C., Aartsma, T. J., Canters, G. W., and Moerner, W. E. (2011) Redox cycling and kinetic analysis of single molecules of solution-phase nitrite reductase. *Proc. Natl. Acad. Sci. U.S.A. 108*, 17269−17274.

(116) Pugh, R. A., Honda, M., and Spies, M. (2010) Ensemble and single-molecule fluorescence-based assays to monitor DNA binding, translocation, and unwinding by iron−sulfur cluster containing helicases. *Methods 51*, 313−321.
(117) Edman, L., FiSldes-Papp, Z., Wennmalm, S., and Rigler, R. (1999) The fluctuating enzyme: A single molecule approach. *Chem. Phys. 247*, 11−22.
(118) Edman, L., and Rigler, R. (2000) Memory landscapes of single-enzyme molecules. *Proc. Natl. Acad. Sci. U.S.A. 97*, 8266−8271.
(119) Cogdell, R. J., Gall, A., and Kohler, J. (2006) The Architecture and Function of the Light-Harvesting Apparatus of Purple Bacteria: From Single Molecules to in vivo Membranes. *Q. Rev. Biophys. 39*, 227−324.
(120) Saga, Y., and Tamiaki, H. (2004) Fluorescence Spectroscopy of Single Photosynthetic Light-Harvesting Supramolecular Systems. *Cell Biochem. Biophys. 40*, 149−165.
(121) Rutkauskas, D., Cogdell, R. J., and van Grondelle, R. (2006) Conformational Relaxation of Single Bacterial Light-Harvesting Complexes. *Biochemistry 45*, 1082−1086.
(122) Loos, D., Cotlet, M., de Schryver, F., Habuchi, S., and Hofkens, J. (2004) Single-Molecule Spectroscopy Selectively Probes Donor and Acceptor Chromophores in the Phycobiliprotein Allophcocyanin. *Biophys. J. 87*, 2598−2608.
(123) de Ruijter, W. P., Oellerich, S., Segura, J. M., Lawless, A. M., Papiz, M., and Aartsma, T. J. (2004) Observation of the Energy-Level Structure of the Low-Light Adapted B800 LH4 Complex by Single-Molecule Spectroscopy. *Biophys. J. 87*, 3413−3420.
(124) Tietz, C., Jelezko, F., Gerken, U., Schuler, S., Schubert, A., Rogl, H., and Wrachtrup, J. (2001) Single Molecule Spectroscopy on the Light-Harvesting Complex II of Higher Plants. *Biophys. J. 81*, 556−562.
(125) van Oijen, A. M., Ketelaars, M., Kohler, J., Aartsma, T. J., and Schmidt, J. (1999) Unraveling the Electronic Structure of Individual Photosynthetic Pigment-Protein Complexes. *Science 285*, 400−402.
(126) Bopp, M. A., Jia, Y., Li, L., Cogdell, R. J., and Hochastrasser, R. M. (1997) Fluorescence and Photobleaching Dynamics of Single Light-Harvesting Complexes. *Proc. Natl. Acad. Sci. U.S.A. 94*, 10630−10635.
(127) Giepmans, B. N. G., Adams, S. R., Ellisman, M. H., and Tsien, R. Y. (2006) The Fluorescent Toolbox for Assessing Protein Location and Function. *Science 312*, 217−224.
(128) Haugland, R. P. (2005) *The Handbook: A Guide to Fluorescent Probes and Labeling Technologies*, Invitrogen Corp.
(129) Ha, T. (2001) Single-Molecule Fluorescence Resonance Energy Transfer. *Methods 25*, 78−86.
(130) Hansen, A. G., Zhang, J., Christensen, H. E. M., Welinder, A. C., Wackerbarth, H., and Ulstrup, J. (2004) Electron transfer and redox metalloenzyme catalysis at the single-molecule level. *Isr. J. Chem. 44*, 89−100.
(131) Zhang, J., Chi, Q., Hansen, A. G., Jensen, P. S., Salvatore, P., and Ulstrup, J. (2012) Interfacial electrochemical electron transfer in biology: Towards the level of the single molecule. *FEBS Lett. 586*, 526−535.
(132) Alessandrini, A., Corni, S., and Facci, P. (2006) Unraveling Single Metalloprotein Electron Transfer by Scanning Probe Techniques. *Phys. Chem. Chem. Phys. 8*, 4383−4397.
(133) Bonanni, B., Andolfi, L., Bizzarri, A. R., and Cannistraro, S. (2007) Functional Metalloproteins Integrated with Conductive Substrates: Detecting Single Molecules and Sensing Individual Recognition Events. *J. Phys. Chem. B 111*, 5062−5075.
(134) Wigginton, N. S., Rosso, K. M., and Hochella, M. F., Jr. (2007) Mechanisms of Electron Transfer in Two Decaheme Cytochromes from a Metal-Reducing Bacterium. *J. Phys. Chem. B 111*, 12857−12864.
(135) Pia, E. A. D., Macdonald, J. E., Elliott, M., and Jones, D. D. (2012) Direct Binding of a Redox Protein for Single-Molecule Electron Transfer Measurements. *Small 8*, 2341−2344.
(136) Bonanni, B., Kamruzzahan, A. S. M., Bizzarri, A. R., Rank, C., Gruber, H. J., Hinterdorfer, P., and Cannistraro, S. (2005) Single Molecule Recognition between Cytochrome C 551 and Gold-Immobilized Azurin by Force Spectroscopy. *Biophys. J. 89*, 2783−2791.
(137) Bonanni, B., Bizzarri, A. R., and Cannistraro, S. (2006) Optimized Biorecognition of Cytochrome c 551 and Azurin Immobilized on Thiol-Terminated Monolayers Assembled on Au(111) Substrates. *J. Phys. Chem. B 110*, 14574−14580.
(138) Tarantaa, M., Bizzarria, A. R., and Cannistraro, S. (2008) Probing the interaction between p53 and the bacterial protein azurin by single molecule force spectroscopy. *J. Mol. Recognit. 21*, 63−70.
(139) Bizzarri, A. R., Santini, S., Coppari, E., Bucciantini, M., Agostino, S. D., Yamada, T., Beattie, C. W., and Cannistraro, S. (2011) Interaction of an anticancer peptide fragment of azurin with p53 and its isolated domains studied by atomic force spectroscopy. *Int. J. Nanomed. 6*, 3011−3019.
(140) Yersin, A., Osada, T., and Ikai, A. (2008) Exploring Transferrin-Receptor Interactions at the Single-Molecule Level. *Biophys. J. 94*, 230−240.
(141) Ikuta, K., Yersin, A., Ikai, A., Aisen, P., and Kohgo, Y. (2010) Characterization of the Interaction between Diferric Transferrin and Transferrin Receptor 2 by Functional Assays and Atomic Force Microscopy. *J. Mol. Biol. 397*, 375−384.
(142) Zheng, P., and Li, H. (2011) Direct Measurements of the Mechanical Stability of Zinc-Thiolate Bonds in Rubredoxin by Single-Molecule Atomic Force Microscopy. *Biophys. J. 101*, 1467−1473.
(143) Zheng, P., Takayama, S.-i. J., Mauk, A. G., and Li, H. (2012) Hydrogen Bond Strength Modulates the Mechanical Strength of Ferric-Thiolate Bonds in Rubredoxin. *J. Am. Chem. Soc. 134*, 4124−4131.
(144) Zhou, X., Andoy, N. M., Liu, G., Choudhary, E., Han, K.-S., Shen, H., and Chen, P. (2012) Quantitative Super-resolution Imaging Uncovers Reactivity Patterns on Single Nanocatalysts. *Nat. Nanotechnol. 7*, 237−241.
(145) Hess, S. T., Girirajan, T. P. K., and Mason, M. D. (2006) Ultra-high resolution imaging by fluorescence photoactivation localization microscopy. *Biophys. J. 91*, 4258−4272.
(146) Betzig, E., Patterson, G. H., Sougrat, R., Lindwasser, O. W., Olenych, S., Bonifacino, J. S., Davidson, M. W., Lippincott-Schwartz, J., and Hess, H. F. (2006) Imaging Intracellular Fluorescent Proteins at Nanometer Resolution. *Science 313*, 1642−1645.
(147) Rust, M. J., Bates, M., and Zhuang, X. (2006) Sub-diffraction-limit imaging by stochastic optical reconstruction microscopy (STORM). *Nat. Methods 3*, 793−796.